Molecular Therapy
Original Article

Enhancer Reprogramming within Pre-existing Topologically Associated Domains Promotes TGF-β-Induced EMT and Cancer Metastasis

Yunbo Qiao,[1,7] Zejian Wang,[2,3,7] Fangzhi Tan,[4,7] Jun Chen,[5,7] Jianxiang Lin,[1] Jie Yang,[3] Hui Li,[3] Xiongjun Wang,[1] Andrej Sali,[6] Liye Zhang,[2] and Guisheng Zhong[2,4]

[1]Precise Genome Engineering Center, School of Life Sciences, Guangzhou University, Guangzhou 510006, China; [2]School of Life Science and Technology, ShanghaiTech University, Shanghai 201210, China; [3]University of Chinese Academy of Sciences, Beijing 100049, China; [4]iHuman Institute, ShanghaiTech University, Shanghai, 201210, China; [5]State Key Laboratory of Medicinal Chemical Biology and College of Life Sciences, Nankai University, 94 Weijin Road, Tianjin 300071, China; [6]Department of Bioengineering and Therapeutic Sciences, Department of Pharmaceutical Chemistry, and California Institute for Quantitative Biosciences, University of California, San Francisco, San Francisco, CA 94158, USA

Transcription growth factor β (TGF-β) signaling-triggered epithelial-to-mesenchymal transition (EMT) process is associated with tumor stemness, metastasis, and chemotherapy resistance. However, the epigenomic basis for TGF-β-induced EMT remains largely unknown. Here we reveal that HDAC1-mediated global histone deacetylation and the gain of specific histone H3 lysine 27 acetylation (H3K27ac)-marked enhancers are essential for the TGF-β-induced EMT process. Enhancers gained upon TGF-β treatment are linked to gene activation of EMT markers and cancer metastasis. Notably, dynamic enhancer gain or loss mainly occurs within pre-existing topologically associated domains (TADs) in epithelial cells, with minimal three-dimensional (3D) genome architecture reorganization. Through motif enrichment analysis of enhancers that are lost or gained upon TGF-β stimulation, we identify FOXA2 as a key factor to activate epithelial-specific enhancer activity, and we also find that TEAD4 forms a complex with SMAD2/3 to mediate TGF-β signaling-triggered mesenchymal enhancer reprogramming. Together, our results implicate that key transcription-factor (TF)-mediated enhancer reprogramming modulates the developmental transition in TGF-β signaling-associated cancer metastasis.

INTRODUCTION

Epithelial-to-mesenchymal transition (EMT) is a cellular process characterized by E-cadherin (*CDH1*) downregulation, in which epithelial cells lose their epithelial junctions and polarity, and acquire a motile mesenchymal phenotype, enabling cell migration and invasion.[1] EMT is crucial for embryonic development and components of carcinogenesis, such as tumor stemness, metastasis, and chemotherapy resistance.[2,3] Activation of the EMT program is comprehensively considered a major driver of cancer malignancy and metastasis,[4,5] and successful identification of the *in vivo* EMT states further emphasizes the essential role of EMT in cancer metastasis.[6]

Transcription growth factor β (TGF-β) signaling transduces through extracellular binding with transmembrane TGF-β receptors and triggers SMAD2/3/4 heterotetrametric complexing and entering into the nucleus to modulate target gene transcription.[7] TGF-β signaling can initiate and maintain EMT in various developmental and pathophysiological processes by activating and integrating context-dependent signaling pathways.[8,9] Accumulating evidence has demonstrated that the TGF-β-driven EMT program initiates and facilitates the acquisition of mesenchymal cell features, tumor invasiveness, and cancer metastasis,[10–12] and blockade of TGF-β remarkably inhibits tumor cell migration and metastases,[13,14] highlighting the importance of the TGF-β-induced manifestation of epithelial plasticity in cancer development. It has been proposed that the intrinsic factors and epigenetic states within the primary tumor cells are crucial for responding to metastatic cues (e.g., TGF-β) and the acquisition of metastatic potential.[15,16] A key transcription factor (TF) FOXA2 has been proposed as an essential tumor suppressor by inhibition of mesenchymal ZEB2 and SLUG transcription.[17,18] However, the epigenomic basis underlying TGF-β-induced EMT and metastasis, as well as epigenetic regulation by key TFs remains largely unknown.

Enhancers are a critical class of regulatory elements that always include clusters of TF binding sites and are frequently occupied by histone H3 lysine 27 acetylation (H3K27ac) and histone H3 lysine

Received 8 February 2020; accepted 27 May 2020;
https://doi.org/10.1016/j.ymthe.2020.05.026.

[7]These authors contributed equally to this work.

Correspondence: Yunbo Qiao, Precise Genome Engineering Center, School of Life Sciences, Guangzhou University, Guangzhou 510006, China.
E-mail: ybqiao@gzhu.edu.cn
Correspondence: Liye Zhang, School of Life Science and Technology, ShanghaiTech University, Shanghai 201210, China.
E-mail: zhangly@shanghaitech.edu.cn
Correspondence: Guisheng Zhong, School of Life Science and Technology, ShanghaiTech University, Shanghai 201210, China.
E-mail: zhongsh@shanghaitech.edu.cn

4 mono-methylation (H3K4me1).[19] The establishment and erasure of proximal and distal enhancers during biological progression contribute to cell-state/stage-specific transcriptional modulation of their target genes and are linked to the rewiring of long-range regulatory architectures.[20,21] Chromatin immunoprecipitation (ChIP) assays have been performed in cancer cell lines or organoid cultured cancer tissues to annotate the enhancer profiles correlated with the degree of epithelial differentiation and metastasis.[6,16,22] However, it is unclear how enhancer usage is involved in the TGF-β-triggered EMT program. In the present study, we profiled the enhancer landscape during TGF-β-induced EMT and identified drastic alterations in enhancer activities. Moreover, the epithelial-specific enhancers are mainly established by FOXA2 to antagonize the TGF-β-induced EMT process, while the TGF-β-responsive mesenchymal-specific enhancers that are regulated by the TEAD4/SMAD complex are associated with cancer cell migration and metastasis. Here we highlight the role of key TFs involved in enhancer reprogramming and precise gene regulation through enhancers. Collectively, our findings indicate that key TF-mediated enhancer reprogramming and the pre-existing chromatin interactions with enhancers promote the acquisition of mesenchymal and metastatic traits during carcinogenesis.

RESULTS

Global Analysis of Enhancer Activities during TGF-β-Induced EMT

To explore the molecular mechanisms underlying TGF-β-induced EMT, we chose a well-established *in vitro* cell model (A549, a human lung adenocarcinoma cell line)[18] and TGF-β-treated AML12 hepatocytes[23] to mimic the TGF-β-triggered morphology, behavior, and intrinsic alterations. As expected, TGF-β treatment triggered a substantial loss of cell junctions and epithelial characteristics (Figures S1A and S1B), accompanied by the downregulation of E-cadherin (encoded by *CDH1*) and upregulation of N-cadherin (encoded by *CDH2*) and fibronectin (encoded by *FN1*) in a time- and dose-dependent manner (Figures S1C and S1D). Histone acetylation is a kind of dynamic turnover modification linked to transcriptional activation during cancer development, differentiation, and progression.[24,25] Therefore, we examined the H3K27ac and histone H3 lysine 9 acetylation (H3K9ac) levels upon TGF-β stimulation, and we found that both histone marks remarkably decreased along with the progressive EMT process by western blot and immunostaining assays (Figures S1E–S1H).

To determine whether TGF-β-induced global histone deacetylation is required for the EMT process, we utilized two histone deacetylase (HDAC) inhibitors, trichostatin A (TSA) and MS-275, to co-stimulate AML12 or A549 cells with TGF-β. Interestingly, HDAC inhibitors prominently blocked the downregulation of H3K27ac levels and reversed the TGF-β-induced morphological, molecular (such as mesenchymal markers *Fn1*, *Vim*, and *Cdh2*), as well as transcriptomic changes in AML12 and A549 cells (Figures S1I–S1M). Moreover, we also found that *HDAC1* depletion, which antagonized TGF-β-triggered EMT (Figures S1N–S1P) as reported previously,[26,27] resulted in the significant upregulation of H3K27ac levels (Figure S1N). Collectively, these results demonstrate that HDAC1-mediated histone deacetylation is required for TGF-β-induced EMT.

To explore the histone modification-linked epigenetic mechanisms underlying the TGF-β-triggered transcriptional program, we generated transcriptome and epigenome data of epithelial A549 cells and TGF-β-induced mesenchymal cells with highly homogeneous cell populations (Figure 1A). RNA sequencing (RNA-seq) analysis showed 785 TGF-β-downregulated genes (epithelial-specific; e.g., *IGFBP1*, *GDF15*, *CDH1*, *FGFBP1*) that were related to epithelial features and 1,285 upregulated genes (mesenchymal-specific; e.g., *CDH1*, *SNAI2*, *VIM*, *ZEB1*), which were mainly associated with adherens junction, cell migration, and EMT (Figure S2A). To examine the genome-wide chromatin alterations during the TGF-β-induced EMT, we performed chromatin precipitation followed by high-throughput sequencing (ChIP-seq) to profile the promoter (histone H3 lysine 4 trimethylation [H3K4me3]) and enhancer (H3K27ac and H3K4me1) activities. We mapped these three kinds of histone modifications around the transcriptional start sties (TSSs; ±3 kb) of differentially expressed genes (DEGs) upon TG-Fβ stimulation. We found that the gene upregulation and downregulation by TGF-β were associated with a minimal increase and decrease in these transcriptionally active modifications in promoters around TSSs, respectively (Figures S2B and S2C).

Subsequently, the number of peaks with gain or loss of detected modifications in a whole-genome comparison during TGF-β-induced EMT was calculated. Intriguingly, the number of regions gaining or losing enhancer peaks occupied by H3K4me1 or H3K27ac during EMT was much higher than that of H3K4me3 peaks enriched at promoters (Figure 1B), indicating that the distal enhancers are more important than promoter activity dynamics for the TGF-β-triggered EMT process. Among the identified 147,077 enhancers that were union from enhancers in A549 and TGF-β treatment groups, the majority of them were poised enhancers marked by H3K4me1 only, while a subset of active enhancers were marked by both H3K4me1 and H3K27ac (Figures 1C and 1D; the peak density for active and poised enhancers was shown as boxplot in Figure S2D). Moreover, the expression of active enhancer-linked genes was higher than poised enhancer-linked genes in both A549 and TGF-β-treated cells (Figure 1E), indicating that enhancer dynamics is essential for TGF-β-triggered transcriptomic alterations. A River plot based on ChromHMM was generated to trace the enhancer dynamics upon TGF-β treatment, demonstrating that the majority of enhancer bins (200-bp bins) were maintained at a poised or active state, and that a small fraction of enhancer bins underwent active-to-poised (e.g., *IGFBP1*, *FGFBP1*, and *FGA*) or poised-to-active (e.g., *WNT7A*, *MMP2*, and *TIMP3*) state transitions, which were associated with epithelial cell characteristics or mesenchymal cell migration, respectively (Figures 1F and S2E). Thus, these data together demonstrate that TGF-β-activated mesenchymal enhancers acquire a pre-adopted poised state in epithelial cancer cells, and that the dynamic regulation of enhancer activities is crucial for the TGF-β-initiated EMT program.

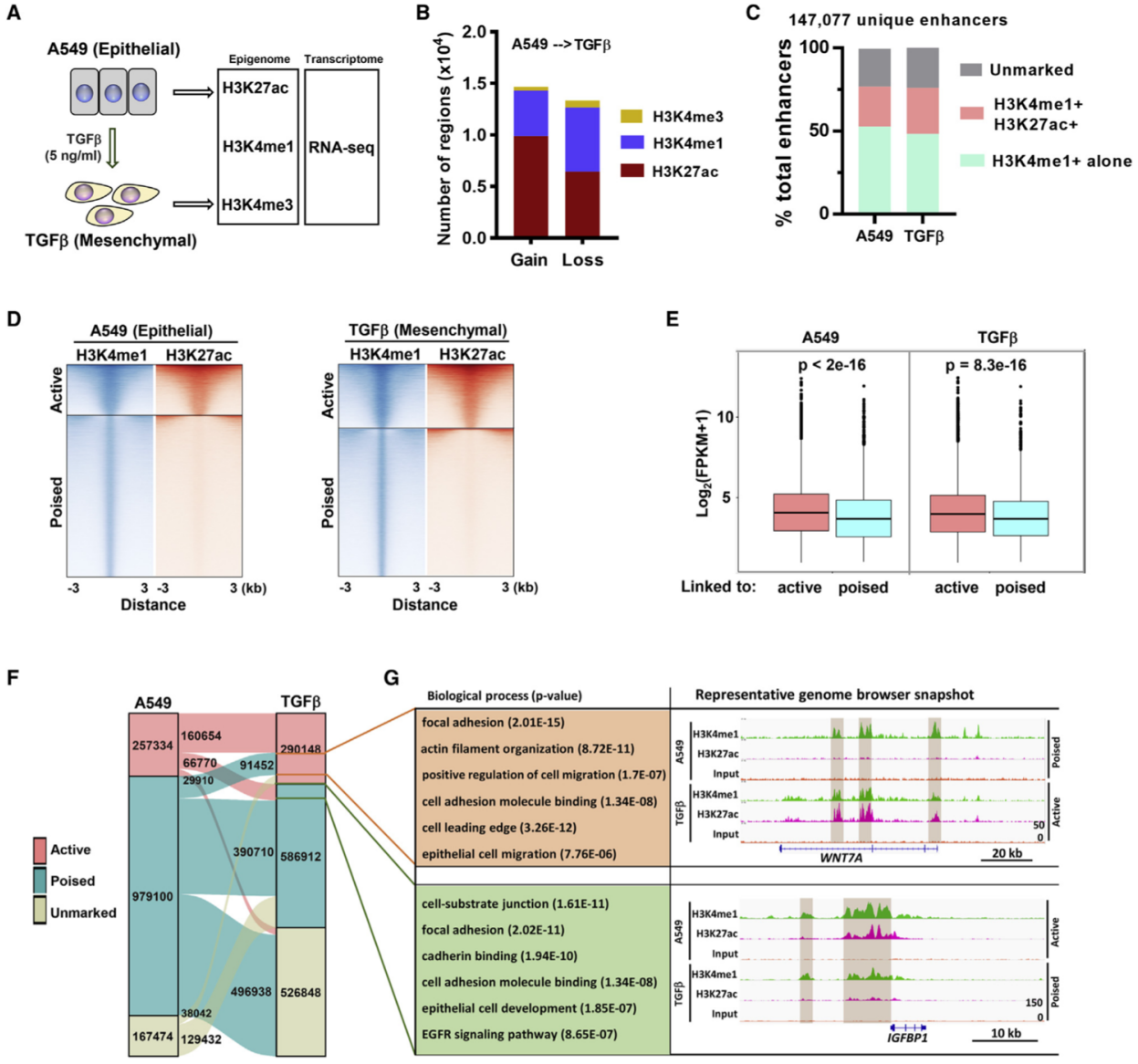

Figure 1. Global Identification of Poised and Active Enhancers during TGF-β-Induced EMT

(A) Schematic for the epigenetic landscaping of TGF-β-induced EMT. Epithelial A549 cells were stimulated with TGF-β (5 ng/mL) for 48 h. A549 and TGF-β-treated cells were subjected to ChIP-seq analysis of H3K27ac, H3K4me1, and H3K4me3 enrichment, as well as RNA-seq analysis, respectively. (B) Bar plot showing the number of peaks by MACS2 that gained or lost indicated modifications during TGF-β-induced EMT. "Gain" or "loss" means the indicated modifications peaks that are specific in TGF-β-treated or untreated conditions, respectively. (C) Total number of candidate enhancer peaks identified during TGF-β-induced EMT categorized by H3K27ac and H3K4me1 deposition combinations by MACS2. Unmarked enhancers in A549 condition means TGF-β-specific enhancers, and unmarked enhancers in TGF-β condition means A549-specific enhancers. (D) Density of normalized ChIP-seq signal for H3K4me1 and H3K27ac modifications relative to midpoint at putative poised and active enhancers in A549 and TGF-β-treated cells. (E) Boxplots of mRNA expression, measured in log2(FPKM+1) at linked genes of poised and active enhancers in A549 and TGF-β-treated cells. FPKM, fragments per kilobase million. *p < 2.2e−16, Wilcoxon rank-sum test. (F) River plot showing the global dynamics of poised and active enhancer regions during TGF-β-induced EMT. ChromHMM software was used to dissect the whole genome into 200-bp bins, and chromatin states were defined according to ChIP-seq signals within each 200-bp bin. Poised enhancer, only H3K4me1 signal; active enhancer, H3K27ac and H3K4me1 positive signals; unmarked, no signal for three ChIP-seq signals. Notably, the enhancers that were retained unmarked during this process were not shown. (G) Gene ontology analysis of poised-to-active and active-to-poised enhancer-linked genes (left panel). Representative genome browser snapshot showing the poised-to-active (*WNT7A*) and active-to-poised (*IGFBP1*) enhancer transition induced by TGF-β for H3K27ac and H3K4me1 ChIP-seq profiles.

Identification of Epithelial- and Mesenchymal-Specific Enhancers Linked to Cancer Metastasis

To explore how the altered enhancer landscape directs transcriptomic programming during EMT progression, we profiled genome-wide enrichment of H3K27ac in mock- and TGF-β-treated A549 cells and identified peaks with >4-fold changes in H3K27ac signals as differentially acetylated peaks. According to this criterion, we recovered 6,013 regions with decreased H3K27ac signals, which we hereafter refer to as epithelial-specific or LOSS enhancers; we also identified 8,956 mesenchymal-specific or GAIN enhancers with increased H3K27ac signals upon TGF-β treatment. LOSS or GAIN enhancer regions were also occupied by H3K4me1, with similar but weaker decreasing or increasing tendencies (Figures 2A and S3A). The reservation of a relatively strong H3K4me1 signal upon TGF-β treatment for LOSS enhancers (Figures 2A and S3A) suggests that TGF-β-induced mesenchymal cells reserve poised enhancers for epithelial-specific genes, which possibly explains the reversible features of the EMT process named mesenchymal-to-epithelial transition (MET).[28]

More than 80% of the GAIN and LOSS regions were distributed outside of the promoter regions (Figure 2B), confirming that these regions represent enhancer elements. For instance, we observed apparent LOSS enhancers in epithelial-specific *CDH1*, *CLDN3*, and *GDF15* genes, as well as GAIN enhancers in *CDH2*, *FN1*, and *SNAI2* in TGF-β-treated cells (Figures 2C and S3B). To screen highly correlated targets with GAIN/LOSS enhancers, we performed the following analyses with an 8-fold change in H3K27ac signals upon TGF-β treatment (Figure S3C). A gene ontology analysis of genes near LOSS enhancers revealed a significant enrichment in epithelial cell functions, whereas the GAIN enhancers nearby genes were mainly associated with cell migration and polarization (Figure 2D). Moreover, we also demonstrated that the TGF-β-downregulated genes with histone deacetylation were mainly related to epithelium development and the apical part of cells (Figure S3D), suggesting that the TGF-β-induced deacetylation contributes to the silencing of epithelial gene expression. Gene set enrichment analysis (GSEA) showed that GAIN enhancer-linked genes were mainly attributed to TGF-β-upregulated genes, whereas the LOSS region nearby genes principally belonged to the TGF-β-downregulated gene set (Figure 2E). Moreover, we overlapped our identified GAIN/LOSS enhancers with that triggered by TGF-β in breast cancer MDA-MB-231 cells,[29] and found a large number of overlapped gained enhancers, but a small number of overlapped lost enhancers (Figure S3E). It suggests that TGF-β-induced gained enhancers are relatively conserved between different types of epithelial cancer cells to generate a similar EMT-triggering program in responding to TGF-β exposure, while the lost enhancers are relatively multiplex, linked to common epithelial cell characteristics (overlapped), as well as cancer-type-specific features (non-overlapped) (Figure S3E). These results demonstrate that TGF-β-triggered enhancer reprogramming is essential for the EMT program.

To explore whether these LOSS/GAIN enhancer-associated genes were associated with cancer metastasis, we analyzed those gene sets in pancreatic ductal adenocarcinoma (PDA) (GEO: GSE71729) datasets[30] and colorectal cancer datasets (GEO: GSE41258).[31,32] For sets of DEGs in PDA between normal and primary/metastatic tissues, we found that GAIN enhancer-linked genes were mainly enriched in primary or metastatic cancer tissues, and the highly expressed DEGs in primary or metastatic tumors were mainly overlapped with TGF-β-upregulated genes (Figure 2F). To further investigate the correlation between GAIN/LOSS enhancer-linked genes with cancer metastasis, we performed pairwise correlation analyses of mRNA expression of GAIN/LOSS enhancer-linked genes in primary and metastatic tumors (GEO: GSE71729 and GSE41258).[30,31] We found that 160 and 190 LOSS enhancer-linked genes were highly expressed in primary PDA and colon cancer tissues, respectively; on the contrary, there were 248 and 251 GAIN enhancer-linked genes upregulated in metastatic tumors, including some known and potent EMT inducers (Figures 2G and S3F). Interestingly, 61 downregulated genes and 56 upregulated genes were overlapped between the two types of cancers during cancer metastasis (Figure S3G). Therefore, subsets of epithelial- and mesenchymal-specific enhancer-associated genes during the TGF-β-induced EMT process are differentially expressed between primary and metastatic tumors, suggesting their potential relevance with cancer metastasis.

TGF-β-Induced Enhancer Alterations Mainly Occur within Pre-existing Topologically Associated Domains (TADs)

Enhancers always act through distal interaction with target promoters; therefore, we performed high-throughput chromosome conformation capture (Hi-C) analysis that can be utilized to characterize the long-range looping interactions, promoter-enhancer contacts, and the three-dimensional (3D) genome architecture alterations.[33] It showed that chromatin interactions were not significantly changed before and after TGF-β treatment at the whole-genome levels (Figures 3A and S4A). However, we found that the interaction strength between GAIN enhancers and TGF-β-upregulated gene promoters was much stronger than that between GAIN enhancers and TGF-β-downregulated gene promoters (Figure 3B, left); on the contrary, the interaction strength between LOSS enhancers and TGF-β-downregulated gene promoters was much stronger than that between LOSS enhancers and TGF-β-upregulated gene promoters (Figure 3B, right). It suggests that the interactions between GAIN enhancers and TGF-β-upregulated gene promoters, as well as LOSS enhancers and TGF-β-downregulated gene promoters, contribute to the differential gene expression upon TGF-β treatment, and the pre-existing interactions between enhancers and promoters of DEGs attribute to the rapid transcriptional response to TGF-β stimulation. We then identified active (A) and inactive (B) compartments using principal-component analysis (PCA) and mapped the transition between A and B among the two samples. The majority of these compartments were maintained in an unchanged state, and only a very small proportion of compartments underwent transitions between A and B (A-to-B: 908; B-to-A: 489), as shown by a River plot (Figure S4B).

Next, we analyzed the normalized enrichment of ChIP-seq signals for H3K27ac and H3K4me1, demonstrating that both enhancer-related histone modifications showed higher enrichment in compartment A versus

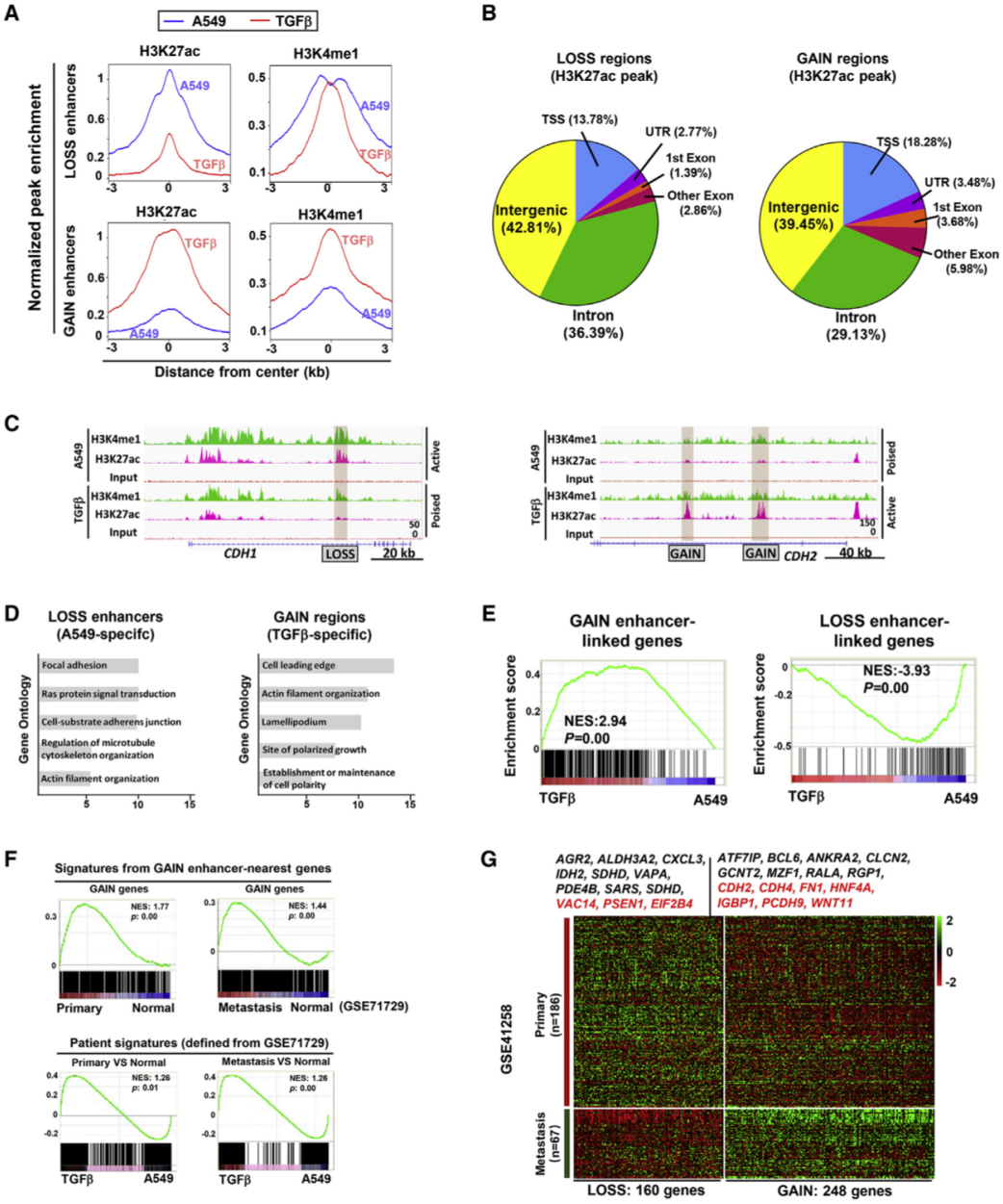

Figure 2. Identification of Epithelial- and Mesenchymal-Specific Enhancers Linked to Cancer Metastasis

(A) Normalized ChIP-seq signals for epithelial-specific (LOSS, n = 6,013) and mesenchymal-specific (GAIN, n = 8,956) H3K27ac peaks, as well as corresponding H3K4me1 peaks relative to midpoint at putative enhancers (6 kb around the center) in A549 and TGF-β-treated cells. The cutoff for GAIN and LOSS enhancers is set as the 4-fold change in H3K27ac peak signals between TGF-β and A549. Peaks are centered on the middle of H3K27ac peaks and ±3-kb region displayed. (B) Pie chart showing the genomic annotations of LOSS and GAIN regions according to the location of a given peak. TSS, "−1 kb to +100 bp" of TSSs; UTR includes both 5′ and 3′ UTRs; 1st exon, the first exon of a coding gene; other exon, the peaks distributed in the exons (not including the first exon). (C) Representative H3K27ac and H3K4me1 ChIP-seq profiles of LOSS (e.g., *CDH1*) and GAIN regions (e.g., *CDH2*) in A549 and TGF-β-treated cells. (D) Enriched Gene Ontology terms for epithelial-specific and mesenchymal-specific enhancers in Figure S3C. (E) Gene set enrichment analysis (GSEA) of TGF-β versus A549 RNA-seq using a signature of GAIN enhancer-linked genes (GAIN genes) or LOSS enhancer-linked genes (LOSS genes). Normalized enrichment score (NES) and nominal p value were provided according to GSEA. (F) GSEA-based comparison of PDA patient-gene expression profiles (GEO: GSE71729: primary versus normal; metastasis versus normal) with a signature of GAIN genes (upper panel). GSEA of TGF-β versus A549 RNA-seq using a signature of patient-derived DEGs (GEO: GSE71729: primary versus normal; metastasis versus normal) (lower panel). (G) Heatmap representation of DEGs between primary and metastasis patients of GEO: GSE41258. The genes marked in red were known EMT markers or epithelial/mesenchymal developmental genes.

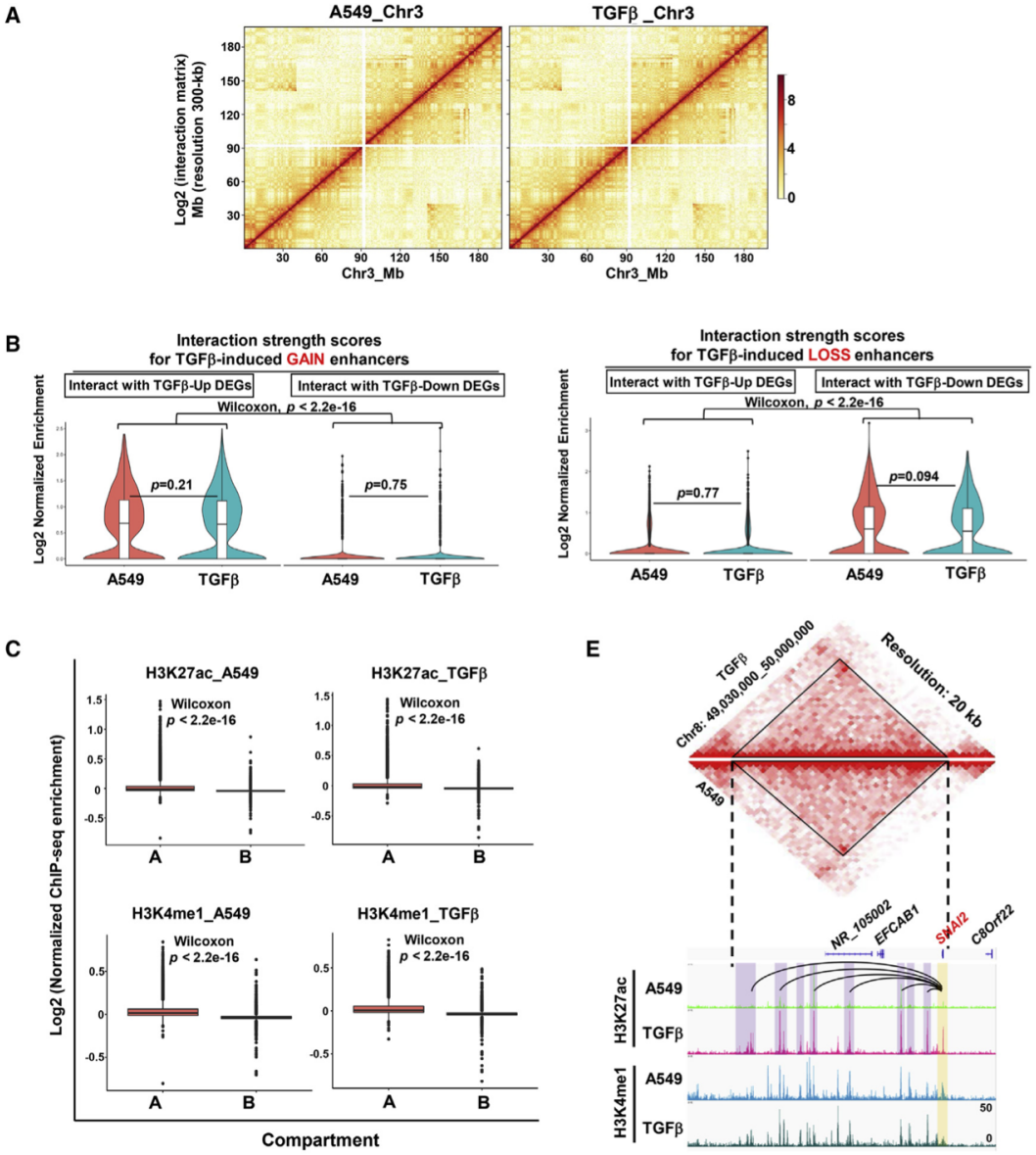

D

	(a) Altered enhancers	(b) Altered enhancers within TADs (linked genes)	(c) TADs with altered enhancers (n=18,671)	(d) Overlapping with altered TADs (n=585)	(e) DEGs covered by TADs with altered enhancers
GAIN	8,956	7,164 (80.0%) (3,212)	3,480 (18.6%)	44 (7.5%)	489-up (n=489/1285, 38.1%)
LOSS	6,013	4,843 (80.5%) (2,404)	2,698 (14.5%)	37 (6.3%)	271-down (=271/785, 34.5%)

Figure 3. Enhancer Reprogramming-Linked 3D Genome Architecture Alterations during TGF-β-Induced EMT

(A) Observed contact matrices for chromosome 3 (chr3) at 300-kb resolution in A549 and TGF-β-treated cells. Scale bar is adjusted to account for the total coverage on chr3 in detected cells. (B) Normalized enrichment for interaction strength scores between the TSS regions (promoters) of TGF-β-induced genes (TGF-β-Up DEGs or TGF-β-Down DEGs) and GAIN or LOSS enhancer regions. Resolution: 5 kb. (C) Normalized ChIP-seq enrichment for H3K27ac or H3K4me1 in compartments A and B for A549 or TGF-

(legend continued on next page)

B (Figure 3C), implying that enhancer enrichment may be required for gene activation in active compartments. Next, we identified 18,671 TADs with HOMER among A549 and TGF-β-treated samples, and revealed that only 585 TADs were significantly different between the two samples ($p < 0.05$) (Figure S4C), indicating that the dynamics of TADs might not be the main contributor to TGF-β-triggered expression changes. We also analyzed the correlation between the enhancer turnover and TAD dynamics, and found that over 80% of GAIN/LOSS enhancers were located within the detected TADs (Figure 3D). In addition, 38.1% of TGF-β-upregulated genes and 34.5% of TGF-β-downregulated genes were located within the TADs with GAIN/LOSS enhancers (Figure 3D). These data suggest that the promoters of TGF-β-responsive targets, such as *SNAI2*, *MMP10*, and *FN1*, are already in contact with their proximal or distal enhancers in epithelial cells before signaling, and the enhancers within TADs were gained upon TGF-β stimulation, resulting in the upregulation of TGF-β-responsive genes; however, the neighboring enhancers out of the TADs were not significantly changed (Figures 3E and S4D). Collectively, our results demonstrate that the enhancer dynamics within TADs with pre-existing contacts, but not TAD or compartment transitions, is the main contributor to TGF-β-induced transcriptome alterations.

FOXA2 Contributes to Epithelial Enhancer Activation

The pre-existing chromatin interactions provide a precondition for enhancer activation and subsequent gene transcription; therefore, identification of key regulators involved in enhancer activation is especially important. To achieve this, we performed MOTIF enrichment analysis for epithelial-specific enhancers that contained clusters of TF binding sites, and revealed the enrichment for a series of TF binding motifs, including *JUNB*, *FOXA2*, *FOXA1*, and *ELF3* motifs (Figure 4A), and some of these TFs, such as *JUNB* and *ELF3*, have well-documented functions in epithelium development.[34,35] RNA-seq profiling showed that the expression of *FOXA2* and *ELF3* was downregulated by TGF-β (Figure S5A). As expected, *FOXA2* expression was positively correlated with epithelial marker genes (especially *CDH1*) in PDA tissues (Figure S5B). Furthermore, loss- or gain-of-function analysis in A549 cells demonstrated that FOXA2 was sufficient for maintaining epithelial characteristics and antagonized TGF-β-induced cell migration and transcriptomic changes (Figures S5C–S5H), which is consistent with a previous report.[18] However, how FOXA2 functions to antagonize TGF-β-induced EMT remains unclear. According to our MOTIF prediction, we reasoned that FOXA2 may act as a key TF to mediate epithelial enhancer activation and to maintain epithelial characteristics.

To test this hypothesis, we performed ChIP-seq analysis in *FOXA2*-knockdown and *FOXA2*-overexpressing A549 cells. Intriguingly, the H3K27ac enrichment for epithelial-specific enhancers was strongly enhanced by *FOXA2* overexpression but decreased by FOXA2 depletion, and the effect of *FOXA2* knockdown on LOSS enhancers was similar to the effect of TGF-β treatment; however, FOXA2 showed no significant effect on GAIN enhancers (Figures 4B and 4C). The genes near FOXA2-mediated LOSS enhancers mainly contributed to mitotic division, transcriptional regulation, and chromatin remodeling (Figure S5I), which might be achieved by FOXA2 functions in enhancer activation, possibly through interaction with a histone acetyl-transferase, P300 (Figure 4D; the direct interaction between FOXA2 and P300 was also confirmed by immunoprecipitation [IP] assays with DNA digestion; data not shown), to mediate loci-specific H3K27ac enrichment. Surprisingly, we overlapped the H3K27ac peaks with FOXA2 binding peaks in A549 cells[36] and revealed that 43.2% of co-occupied enhancers belonged to LOSS enhancers (n = 1,656; 8-fold cutoff) (Figure 4E). Interestingly, rare FOXA2 binding peaks were overlapped with GAIN enhancers (data not shown). Subsequently, the FOXA2 and LOSS-H3K27ac co-occupied genes were compared with TGF-β-downregulated genes, revealing 177 overlapping genes, which include a cluster of epithelial marker genes (Figure 4F), such as *CDH1* and *GDF15*. The H3K27ac enrichment in these genes was decreased by FOXA2 knockdown but increased by FOXA2 overexpression, and these H3K27ac enrichment loci were also co-bound by FOXA2 (Figure 4G). Although the functions of FOXA2 were consistent with a previous study in breast cancer,[17] we first revealed its roles in maintaining epithelial enhancer activities. These results demonstrate that FOXA2 acts as a key TF to maintain epithelial enhancer activities, and TGF-β-triggered FOXA2 downregulation promotes cancer cell migration.

TEAD2/4 Mediates TGF-β-Induced Mesenchymal Enhancer Reprogramming

Next, we performed MOTIF analysis for GAIN enhancers, and the intracellular mediators of TGF-β signaling, SMAD2/3/4, were observed in the top list (p value) of predicted TFs with their potential binding sites within GAIN enhancers (Figure 5A). Interestingly, the transcriptional effectors of the Hippo signaling pathway, TEAD2 and TEAD4, were also found among the GAIN enhancer-predicted TFs (Figure 5A). To test whether SMAD2/3/4 or TEAD2/4 can co-bind to the gained enhancers, we overlapped the gained H3K27ac peaks (Figure 2A) with binding peaks (defined by MACS2) of TEAD4 (ENCODE project: ENCSR000BUD) and SMAD3 (GSE51510) in TGF-β-treated A549 cells,[37] and 333 co-enrichment peaks were obtained (statistically significant with $p < 2.2 \times 10^{-16}$ based on Fisher's exact test; Figure 5B). This indicates that these gained enhancers might be co-regulated by SMAD and TEAD. Thus, we hypothesized that SMAD may interact with TEAD to mediate TGF-β signaling-triggered EMT. As expected, a co-immunoprecipitation (coIP) assay demonstrated that SMAD2 and

β-treated samples separately. A/B compartments were identified by HOMER with 40-kb resolution. (D) Comparison of GAIN/LOSS enhancers with HOMER-identified TADs. (a) The number of GAIN/LOSS enhancers induced by TGF-β; (b) the number/percentage of GAIN/LOSS enhancers within TADs, as well as the number of these enhancers-linked genes; (c) the number/percentage of TADs with GAIN/LOSS enhancers; (d) the number/percentage of overlapped TADs between TADs with GAIN/LOSS enhancers and 585 differential TADs ($p < 0.05$); and (e) the number/percentage of DEGs overlapped with altered enhancer containing TAD-linked genes were calculated. (E) Hi-C contact maps at the *SNAI2* neighboring regions within an apparent TAD (chr8: 49,030,000–50,000,000). The Integrative Genomics Viewer (IGV) views of ChIP-seq enrichment for H3K27ac and H3K4me1 in A549 and TGF-β-treated cells were shown at the lower panel. The potential interactions or contacts between *SNAI2* and proximal GAIN enhancers were depicted.

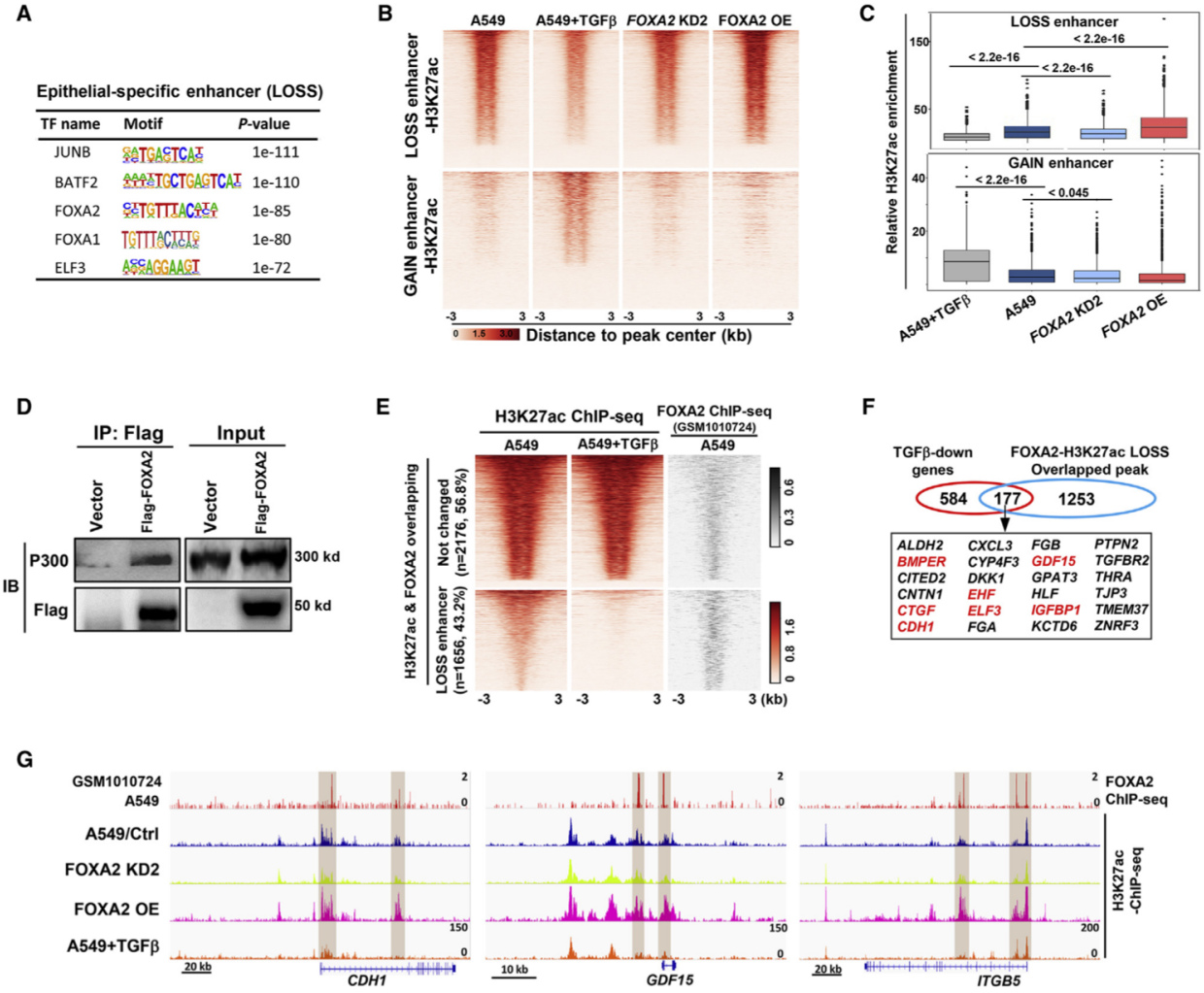

Figure 4. LOSS Enhancer-Predicted Transcription Factors Are Associated with Epithelial-Specific Enhancer Maintenance and Metastasis

(A) Enriched TF binding motifs with associated p values for LOSS enhancers identified by HOMER. (B) Heatmap illustration of H3K27ac peaks signal of LOSS and GAIN enhancers in the indicated groups. In the A549 and A549+TGF-β groups, A549 refers to A549 cells expressing shRNA control. (C) Boxplots showing the relative enrichment of H3K27ac modifications for LOSS and GAIN enhancers, respectively, in A549, TGF-β-treated, *FOXA2* KD2, and *FOXA2* overexpressing (OE) cells. p value calculated by Wilcox test. (D) Immunoprecipitation (IP) was performed with anti-FLAG in vector (GFP) or FLAG-FOXA2-overexpressed A549 cells. The precipitated products were subjected to western blot analysis of P300 and FLAG-FOXA2 expression by using anti-P300 or anti-FLAG antibodies. (E) The H3K27ac peaks were overlapped with FOXA2 binding peaks (GSM1010724) in A549 cells. Then the overlapped H3K27ac and FOXA2 peaks were presented as two groups upon TGF-β treatment: peak not changed (n = 2,176) and peak LOSS (n = 1,656). (F) Venn diagram to compare the TGF-β-downregulated genes and the FOXA2 and H3K27ac co-occupied LOSS enhancer-linked genes. Representative overlapped genes were presented as red color. (G) Representative H3K27ac ChIP-seq profiles of LOSS enhancers around the *CDH1* and *GDF15*, which were regulated by *FOXA2* knockdown or overexpression in A549 cells, and were co-occupied by H3K27ac, as well as FOXA2 (GSM1010724).

SMAD3 interacted with TEAD4 under TGF-β stimulation (Figures 5C and S6B). Correlation analysis in PDA samples showed that TEAD2/4 expression was positively correlated with the expression of mesenchymal markers (e.g., *ZEB1*, *VIM*, and *SNAI2*) but negatively correlated with epithelial marker genes, as well as *FOXA2* (Figure S6A).

Then we screened two effective short hairpin RNAs (shRNAs) for *TEAD2* and *TEAD4* knockdown, respectively, in HEK293T cells (Figure S6C). We combined dual shRNAs together, resulting in higher knockdown efficiency in A549 cell for both genes (Figures S6C and S6D). As expected, knockdown of *TEAD2* and *TEAD4* separately or together exerted inhibitory effects on TGF-β-induced mesenchymal morphogenesis (Figure S6E) and marker gene expression (Figure 5D). RNA-seq analysis revealed that the upregulation of 394 genes induced by TGF-β was notably blocked by *TEAD2/4* knockdown, whereas their effects on TGF-β-triggered gene downregulation were much more minor (Figure S6F).

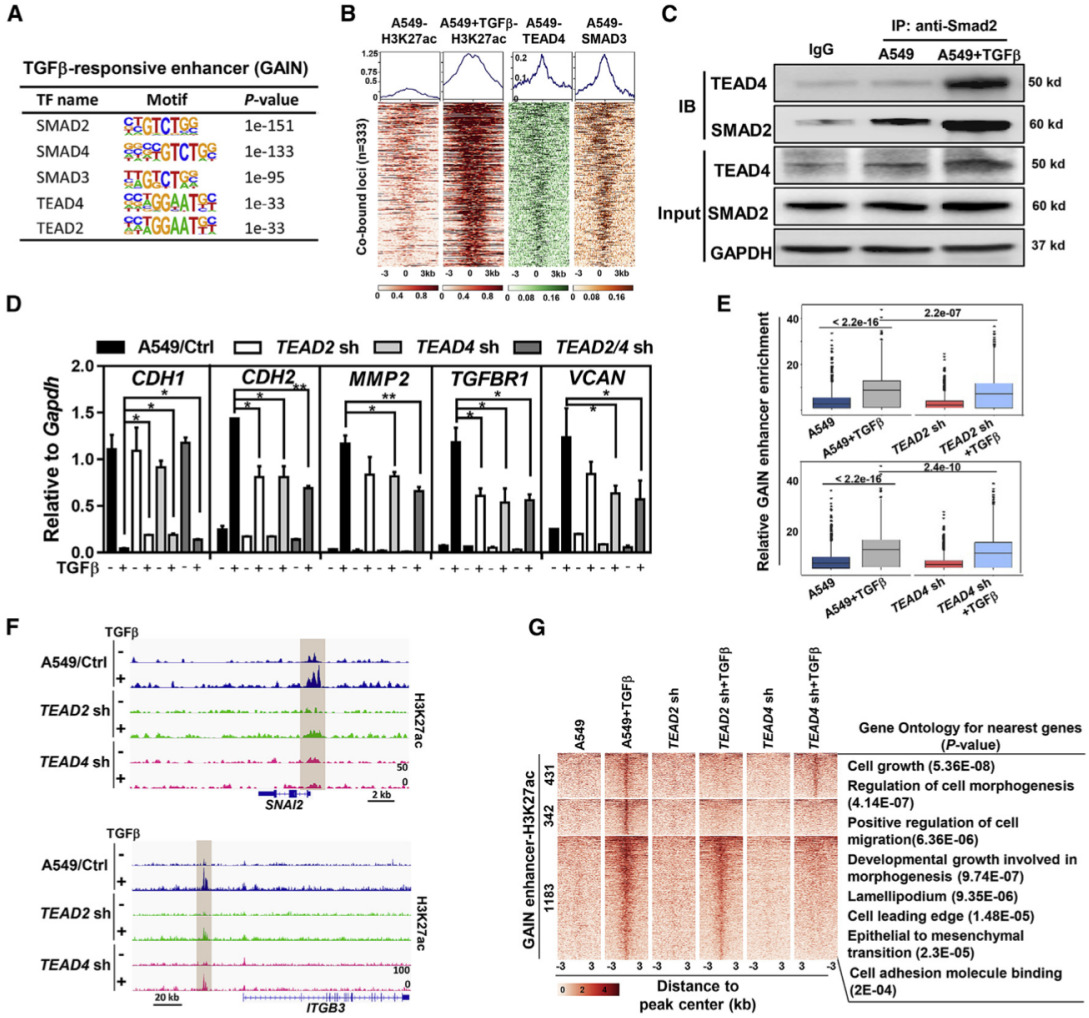

Figure 5. TEAD2/4 Are Required for Mesenchymal-Specific Enhancer Activation in TGF-β-Induced EMT

(A) Enriched TF binding motifs with associated p values for GAIN enhancers identified by HOMER. (B) Heatmap showing the enrichment of 333 gained enhancers, as well as co-enrichment of TEAD4 (ENCODE project: ENCSR000BUD) and SMAD3 (GEO: GSE51510) in A549 cells treated with TGF-β. The gained enhancers in Figure 2A were overlapped with binding peaks of anti-TEAD4 and anti-SMAD3 (defined by MACS2), and 333 overlapped peaks were obtained and presented here. (C) IP analysis of protein interaction between TEAD4 and SMAD2 upon TGF-β treatment by using an anti-Smad2 antibody. The precipitated products were subjected to western blot analysis of TEAD4 and SMAD2 expression. Rabbit IgG served as a negative control. (D) Quantitative real-time PCR analysis of *CDH1*, *CDH2*, *MMP2*, *TGFBR1*, and *VCAN* expression in A549 cells expressing control or *TEAD2* sh, *TEAD4* sh, or *TEAD2/4* sh with or without TGF-β treatment. (E) Boxplots showing the relative enrichment of H3K27ac modifications for GAIN enhancers in the indicated experimental groups. p value calculated by Wilcox test. (F) Representative H3K27ac ChIP-seq profiles of GAIN enhancers around the *SNAI2* and *ITGB3* in *TEAD2/4* knockdown cells. (G) Heatmap showing the GAIN enhancers induced by TGF-β treatment, which were lost or impaired in *TEAD2* and/or *TEAD4* knockdown cells. Gene Ontology terms for the nearest genes for these differentially regulated enhancers by *TEAD2/4* were also presented. IB, immunoblot.

Together, these data suggest that TEAD2 and TEAD4 are involved in TGF-β-triggered mesenchymal gene activation during EMT progression.

More importantly, TEAD2/4 depletion resulted in a modest but significant decrease in GAIN enhancer enrichment in A549 or TGF-β-treated cells (expressing control shRNAs) compared with TEAD2/4 knockdown cells without or with TGF-β treatment (Figures 5E and S6G). For instance, the H3K27ac enrichment in the EMT inducers *SNAI2* and *ITGB3*, which was increased by TGF-β, was significantly impaired in *TEAD2*- and *TEAD4*-depleted cells (Figure 5F). Detailed profiling identified 431 and 1,183 mesenchymal enhancers that were mainly mediated by TEAD2 or TEAD4 separately, as well as 342 overlapping enhancers markedly regulated by both TEAD2 and TEAD4. The genes linked to these TEAD2/4-mediated enhancers were involved in cell morphogenesis, migration, and EMT (Figure 5G). Kaplan-Meier survival analysis showed that higher *TEAD2*

or *TEAD4* expression in lung and liver cancers predicted poor survival rates (Figures S6H and S6I). Thus, we demonstrate that the Hippo signaling mediators TEAD2 and TEAD4 may partially mediate the TGF-β-triggered mesenchymal enhancer activation, possibly through interaction with the SMAD complex to promote cancer progression.

DISCUSSION

During the TGF-β-induced EMT program, we reveal a pre-marked poised state and a pre-existing chromatin interaction within the same TADs between enhancers and mesenchymal regulators in epithelial cells, which is required for mesenchymal enhancer activation. Moreover, the epithelial- and mesenchymal-specific enhancers are maintained or established by crucial TFs, such as FOXA2 and TEAD2/4, respectively. Our data thus provide an epigenetic basis for the EMT progression that is linked to cancer metastasis.

It has been proposed that metastatic cancer transitions are frequently accompanied by massive and recurrent alterations in enhancer activities.[16] For the metastatic process triggered by TGF-β, massive enhancer dynamics (Figures 1 and 2) and HDAC1-mediated histone de-modifications at global levels (Figure S1) have been observed here, highlighting the importance of epigenetic state transitions for carcinogenesis. Interestingly, histone deacetylase inhibitors have been applied in cancer therapy,[38] possibly through blocking the EMT process (Figure S1). Importantly, the acquisition of mesenchymal competence in epithelial-like cancer cells through poising mesenchymal-specific enhancers (Figures 1 and 2) is crucial for maintaining epithelial cells responsive to EMT-inducing signals, such as TGF-β signaling. Moreover, compared with the remarkable transition of active enhancers marked by H3K27ac, the activities of the H3K4me3-marked promoters undergo minor changes (Figure 1B), further indicating that the enhancer usage turnover plays a dominant role during TGF-β-triggered EMT. It is worthy noticing that the global reduction of active enhancer marks (Figure 1C) does not correlate with a global reduction of gene expression, possibly because of differential basal acetylation levels for a different set of genes and other histone modifications involved. Therefore, it is of interest to elucidate the origin of poised mesenchymal-specific enhancers in epithelial cancer cells that are acquired before or during cancer transformation from normal cells. Certainly, accompanying the TGF-β-triggered silencing of epithelial marker genes, the epithelial-specific enhancers transit from an active to poised state (Figures 1 and 2), suggesting that the TGF-β-induced mesenchymal cells might be in a reversible epigenetic state and are able to undergo the MET process, providing a reasonable explanation for the metastasis-associated MET program from an epigenetic view.[39] It is possible that TGF-β-induced mesenchymal cells in a poised state for epithelial genes reverse to an active state during metastasis, facilitating secondary tumorigenesis and colonization.[28] The loss of epithelial-specific enhancers upon TGF-β stimulation initiates the inactivation of epithelial-specific genes and cell-cell adhesion molecule E-cadherin, and promotes the loss of epithelial cell characteristics and the acquisition of motility features (Figure 2), facilitating subsequent metastasis-related events, such as stromal infiltration.[40,41]

The epigenetic priming of cell-type-specific enhancers prior to gene activation helps to explain the highly context-dependent activity of TFs in cellular programming and reprogramming. Specifically, our findings suggest that epithelial-specific TFs, particularly FOXA2, play important roles in maintaining active epithelial-specific enhancers. Loss of these epithelial-specific TFs transforms the active enhancers into poised states for epithelial marker genes (Figure 4) and maintains the ability of cells to reverse into an epithelial-like state. FOXA2 may play differential roles comparing with another forkhead TF FOXA1, although the function of FOXA2 in carcinogenesis sometimes displays in a context-dependent manner.[42]

Loss of epithelial characteristics is a prerequisite for the acquisition of mesenchymal or metastatic traits. We first demonstrate that many mesenchymal marker genes are pre-marked by H3K4me1 without H3K27ac in a poised state (Figure 3), indicating that epithelial cancer cells are capable of activating mesenchymal genes immediately after TGF-β-triggered enhancer reprogramming. In this study, we focused on the acquisition of H3K27ac enhancers in response to TGF-β stimulation. Through functional and profiling analysis, we propose that a series of TFs, such as TEAD2/4, is partially required for TGF-β-induced mesenchymal enhancer activation through interacting with the intracellular mediators of TGF-β signaling, SMAD2/3/4 (Figure 5). Considering the observation that TEAD4 interacts with SMAD2/3 depending on TGF-β stimulation (Figure 5B), we presume that the GAIN enhancer-bound TFs, such as TEAD2/4, can interact only with the phosphorylated SMAD complex in the nucleus and activate mesenchymal enhancers. It has been proposed that the Hippo pathway (TAZ/YAP/TEAD) associates with the TGF-β pathway (SMAD2/3) and/or OCT4 to regulate pluripotency and mesendoderm gene expression during human embryonic stem cell differentiation.[43,44] Here, we identify the SMAD/TEAD complex acting downstream of TGF-β, implying a crosstalk between Hippo and TGF-β signaling in cancer metastasis. It also suggests that SMAD may form a complex with distinct TFs to promote different sets of mesenchymal enhancer activation, resulting in substantial mesenchymal gene activation in response to TGF-β. Consistently, YAP/TEAD has been recently proposed to be required for activation of estrogen-regulated enhancers to promote breast carcinogenesis.[45] To address distal enhancer interactions, we mapped the 3D chromatin structures during TGF-β-induced EMT, and revealed that GAIN and LOSS enhancers are associated with the distal interactions within the TADs for upregulated and downregulated genes, respectively (Figure 3), further demonstrating that enhancer reprogramming promotes the TGF-β-induced EMT through pre-existing chromatin contacts.

In summary, we propose a model for epigenetic regulation in the TGF-β-induced EMT (Figure 6). Epithelial features of cancer cells are maintained by epithelial-specific enhancer-driven gene expression, which is achieved by FOXA2 and P300 complex to sustain H3K27ac modifications. Meanwhile, epithelial marker genes are silenced by the HDAC1-mediated active-to-poised histone

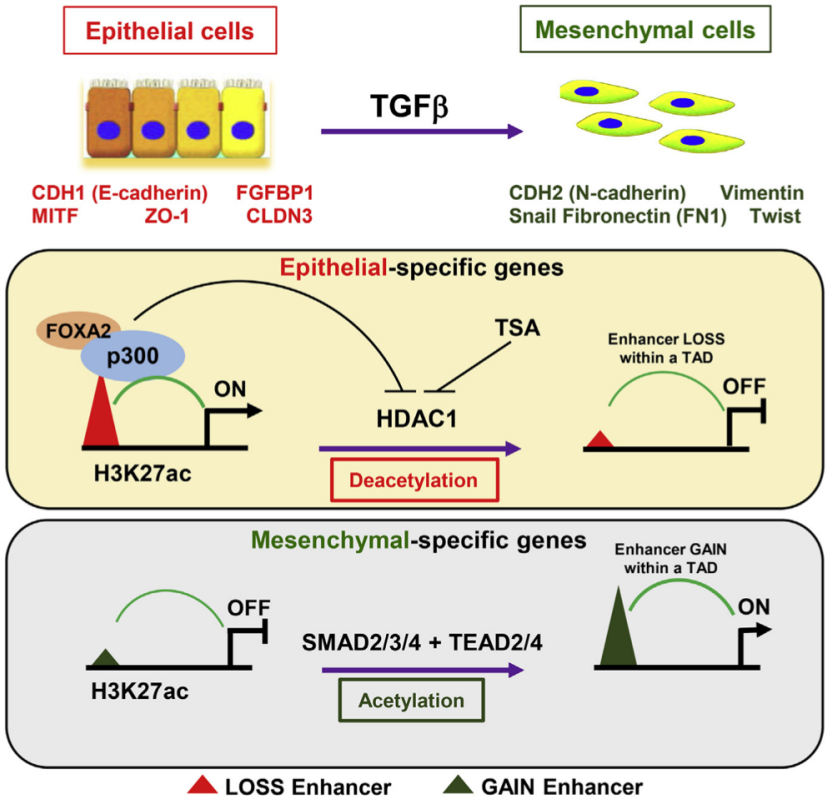

Figure 6. Hypothetical Model for Enhancer Reprogramming in TGF-β-Induced EMT

During the acquisition of mesenchymal features during TGF-β-induced EMT, accompanied with the down-regulation of epithelial-specific genes and upregulation of mesenchymal-specific genes. (1) Epithelial-specific gene activation is controlled by H3K27ac-marked enhancers, which are maintained by P300 and key TFs (e.g., FOXA2) interaction. Upon TGF-β stimulation, FOXA2 is down-regulated and the epithelial-specific enhancers are transited into a poised state, with the decreased interaction strength between epithelial-specific enhancers and promoters within the same TADs. The loss of these enhancers is mediated by HDAC1-linked histone deacetylation, and an HDAC inhibitor TSA can block this process to antagonize TGF-β-induced EMT. (2) The gained mesenchymal-specific enhancers are activated by SMAD2/3/4 and TEAD2/4 complex upon TGF-β treatment, and the chromatin contacts between mesenchymal-specific enhancers and promoters pre-existed within the same TADs, with stronger interaction strength in TGF-β-induced mesenchymal state.

deacetylation, and this process can be blocked by HDAC inhibition. For the acquisition of mesenchymal traits, SMAD and TEAD form a complex in response to TGF-β signaling to promote mesenchymal enhancer activation and gene activation. Thus, TGF-β signaling-triggered enhancer reprogramming is modulated at multiple layers by key TFs and chromatin architectures to regulate cell migration and cancer metastasis. Our study provides an epigenetic insight for understanding EMT and cancer metastasis.

MATERIALS AND METHODS

Cell Culture and Reagents

The human lung cancer epithelial-like A549 cells, mouse hepatocyte AML12 cells, and HEK293T cells used in the present study were originally purchased from American Type Culture Collection. A549 cells were authenticated by mutations contained within our sequencing data by comparing with the COSMIC (Catalogue of Somatic Mutations in Cancer) database. 293T and A549 cells were cultured in Dulbecco's modified Eagle's medium (DMEM) containing 10% fetal bovine serum (FBS) supplemented with penicillin (100 U/mL) and streptomycin (100 μg/mL). AML-12 cells were grown in a 1:1 mixture of DMEM and Ham's F12 medium containing 10% FBS and supplemented with dexamethasone (40 ng/mL), insulin-transferrin-selenium-X, penicillin (100 U/mL), and streptomycin (100 mg/mL). All of these cells were incubated in a humidified atmosphere of 5% CO_2 at 37°C. TSA and MS-275 were purchased from (Medchemexpress, NJ, USA). Recombinant human TGF-β1 (7754-BH-005; R&D) was used to induce the EMT process.

Wound Healing Assays

Confluent A549 monolayers cells were scraped in an approximately 600-μm-wide strip of the cells using a standard 1000-μL pipette tip. Then the wounded monolayers were washed twice to remove nonadherent cells. The wound healing process was captured by phase-contrast microscopy every day for 4 days, and the gap between the wound edges was quantified to calculate the average cell migration speed. Three repeats were performed for each group of experiments.

Western Blot Analysis, Immunostaining, IP Assay, Quantitative Real-Time PCR, and Lentiviral Transduction

The detailed methods for western blot analysis, immunostaining, IP assays, quantitative real-time PCR analysis, and lentiviral transduction were described in the Supplemental Materials and Methods. The shRNA sequences are listed in Table S1. The primer sequences are listed in Table S2.

RNA-Seq, ChIP-Seq, and Hi-C Datasets

The methods and analysis for RNA-seq, ChIP-seq, and Hi-C were described in the Supplemental Materials and Methods. RNA-seq, ChIP-seq, and Hi-C data can be accessed under the Genome Sequence Archive (GSA: CRA001325; https://bigd.big.ac.cn/gsa/). Two replicates for RNA-seq and Hi-C data were presented, and one replicate for ChIP-seq data was provided, which showed highly similar patterns with MDA-MB-231 cells in responding to TGF-β.[29] The downloaded datasets used in this study are listed in Table S3.

Kaplan-Meier Survival Analysis

Kaplan-Meier survival analyses were performed using an online tool named as Kaplan Meier plotter (http://kmplot.com/analysis/) with default parameters.

Statistical Analysis

Quantitative data are presented as means ± SD. Statistical significance was determined by the Student's t test to compare two experimental groups. At least three repeated experiments were performed for statistical analysis: *$p < 0.05$, **$p < 0.01$, ***$p < 0.001$, ****$p < 0.0001$. For boxplot analysis of RNA-seq gene expression or H3K27ac enrichment, the Wilcoxon test was performed.

SUPPLEMENTAL INFORMATION

Supplemental Information can be found online at https://doi.org/10.1016/j.ymthe.2020.05.026.

AUTHOR CONTRIBUTIONS

Y.Q., F.T., and J.C. designed, conceived, and performed the experiments and co-wrote the manuscript. Z.W. and L.Z. performed computational analysis. J.L., J.Y., H.L., A.S., and X.W. performed and helped with the experiments. Y.Q, L.Z., and G.Z. designed, conceived, and supervised the work and co-wrote the manuscript.

CONFLICTS OF INTEREST

The authors declare no competing interests.

ACKNOWLEDGMENTS

We are thankful to all members and authors for important contributions and critical review of the figures and analyses. We thank Prof. Xingxu Huang for critical discussions during this project. This work was supported by the National Key Research and Development Program of China (2018YFC1004700 to Y.Q., 2016YFC0905900 and 2017YFC1001300 to G.Z., and 2018YFC1004602 to L.Z.); The 2015 Thousand Youth Talents Plan of China (G.Z.); the National Natural Science Foundation of China (31771130 to G.Z., 31871332 to L.Z., 31601185 to F.T., and 31701284 to J.C.); and Excellent Youth Foundation of Guangdong Scientific Committee (2020B1515020018 to Y.Q.). We would like to thank the support from the HPC platform of ShanghaiTech University.

REFERENCES

1. Skrypek, N., Goossens, S., De Smedt, E., Vandamme, N., and Berx, G. (2017). Epithelial-to-Mesenchymal Transition: Epigenetic Reprogramming Driving Cellular Plasticity. Trends Genet. *33*, 943–959.
2. Nieto, M.A., Huang, R.Y., Jackson, R.A., and Thiery, J.P. (2016). Emt: 2016. Cell *166*, 21–45.
3. Puisieux, A., Brabletz, T., and Caramel, J. (2014). Oncogenic roles of EMT-inducing transcription factors. Nat. Cell Biol. *16*, 488–494.
4. Krebs, A.M., Mitschke, J., Lasierra Losada, M., Schmalhofer, O., Boerries, M., Busch, H., Boettcher, M., Mougiakakos, D., Reichardt, W., Bronsert, P., et al. (2017). The EMT-activator Zeb1 is a key factor for cell plasticity and promotes metastasis in pancreatic cancer. Nat. Cell Biol. *19*, 518–529.
5. Kalluri, R., and Weinberg, R.A. (2009). The basics of epithelial-mesenchymal transition. J. Clin. Invest. *119*, 1420–1428.
6. Pastushenko, I., Brisebarre, A., Sifrim, A., Fioramonti, M., Revenco, T., Boumahdi, S., Van Keymeulen, A., Brown, D., Moers, V., Lemaire, S., et al. (2018). Identification of the tumour transition states occurring during EMT. Nature *556*, 463–468.
7. Roberts, A.B., Tian, F., Byfield, S.D., Stuelten, C., Ooshima, A., Saika, S., and Flanders, K.C. (2006). Smad3 is key to TGF-beta-mediated epithelial-to-mesenchymal transition, fibrosis, tumor suppression and metastasis. Cytokine Growth Factor Rev. *17*, 19–27.
8. Zavadil, J., and Böttinger, E.P. (2005). TGF-beta and epithelial-to-mesenchymal transitions. Oncogene *24*, 5764–5774.
9. Siegel, P.M., and Massagué, J. (2003). Cytostatic and apoptotic actions of TGF-beta in homeostasis and cancer. Nat. Rev. Cancer *3*, 807–821.
10. Calon, A., Espinet, E., Palomo-Ponce, S., Tauriello, D.V., Iglesias, M., Céspedes, M.V., Sevillano, M., Nadal, C., Jung, P., Zhang, X.H., et al. (2012). Dependency of colorectal cancer on a TGF-β-driven program in stromal cells for metastasis initiation. Cancer Cell *22*, 571–584.
11. Derynck, R., Akhurst, R.J., and Balmain, A. (2001). TGF-beta signaling in tumor suppression and cancer progression. Nat. Genet. *29*, 117–129.
12. Seoane, J., and Gomis, R.R. (2017). TGF-β Family Signaling in Tumor Suppression and Cancer Progression. Cold Spring Harb. Perspect. Biol. *9*, a022277.
13. Muraoka, R.S., Dumont, N., Ritter, C.A., Dugger, T.C., Brantley, D.M., Chen, J., Easterly, E., Roebuck, L.R., Ryan, S., Gotwals, P.J., et al. (2002). Blockade of TGF-beta inhibits mammary tumor cell viability, migration, and metastases. J. Clin. Invest. *109*, 1551–1559.
14. Yang, Y.A., Dukhanina, O., Tang, B., Mamura, M., Letterio, J.J., MacGregor, J., Patel, S.C., Khozin, S., Liu, Z.Y., Green, J., et al. (2002). Lifetime exposure to a soluble TGF-beta antagonist protects mice against metastasis without adverse side effects. J. Clin. Invest. *109*, 1607–1615.
15. Omura, N., and Goggins, M. (2009). Epigenetics and epigenetic alterations in pancreatic cancer. Int. J. Clin. Exp. Pathol. *2*, 310–326.
16. Roe, J.-S., Hwang, C.-I., Somerville, T.D.D., Milazzo, J.P., Lee, E.J., Da Silva, B., Maiorino, L., Tiriac, H., Young, C.M., Miyabayashi, K., et al. (2017). Enhancer reprogramming promotes pancreatic cancer metastasis. Cell *170*, 875–888.e20.
17. Zhang, Z., Yang, C., Gao, W., Chen, T., Qian, T., Hu, J., and Tan, Y. (2015). FOXA2 attenuates the epithelial to mesenchymal transition by regulating the transcription of E-cadherin and ZEB2 in human breast cancer. Cancer Lett. *361*, 240–250.
18. Tang, Y., Shu, G., Yuan, X., Jing, N., and Song, J. (2011). FOXA2 functions as a suppressor of tumor metastasis by inhibition of epithelial-to-mesenchymal transition in human lung cancers. Cell Res. *21*, 316–326.
19. Long, H.K., Prescott, S.L., and Wysocka, J. (2016). Ever-Changing Landscapes: Transcriptional Enhancers in Development and Evolution. Cell *167*, 1170–1187.
20. Guo, Y., Xu, Q., Canzio, D., Shou, J., Li, J., Gorkin, D.U., Jung, I., Wu, H., Zhai, Y., Tang, Y., et al. (2015). CRISPR Inversion of CTCF Sites Alters Genome Topology and Enhancer/Promoter Function. Cell *162*, 900–910.
21. Lupiáñez, D.G., Kraft, K., Heinrich, V., Krawitz, P., Brancati, F., Klopocki, E., Horn, D., Kayserili, H., Opitz, J.M., Laxova, R., et al. (2015). Disruptions of topological chromatin domains cause pathogenic rewiring of gene-enhancer interactions. Cell *161*, 1012–1025.
22. Diaferia, G.R., Balestrieri, C., Prosperini, E., Nicoli, P., Spaggiari, P., Zerbi, A., and Natoli, G. (2016). Dissection of transcriptional and cis-regulatory control of differentiation in human pancreatic cancer. EMBO J. *35*, 595–617.
23. Yamashita, M., Fatyol, K., Jin, C., Wang, X., Liu, Z., and Zhang, Y.E. (2008). TRAF6 mediates Smad-independent activation of JNK and p38 by TGF-beta. Mol. Cell *31*, 918–924.
24. Clayton, A.L., Hazzalin, C.A., and Mahadevan, L.C. (2006). Enhanced histone acetylation and transcription: a dynamic perspective. Mol. Cell *23*, 289–296.
25. Qiao, Y., Wang, R., Yang, X., Tang, K., and Jing, N. (2015). Dual roles of histone H3 lysine 9 acetylation in human embryonic stem cell pluripotency and neural differentiation. J. Biol. Chem. *290*, 9949.
26. Xu, J., Lamouille, S., and Derynck, R. (2009). TGF-beta-induced epithelial to mesenchymal transition. Cell Res. *19*, 156–172.

27. Lei, W., Zhang, K., Pan, X., Hu, Y., Wang, D., Yuan, X., Shu, G., and Song, J. (2010). Histone deacetylase 1 is required for transforming growth factor-beta1-induced epithelial-mesenchymal transition. Int. J. Biochem. Cell Biol. *42*, 1489–1497.

28. Gunasinghe, N.P., Wells, A., Thompson, E.W., and Hugo, H.J. (2012). Mesenchymal-epithelial transition (MET) as a mechanism for metastatic colonisation in breast cancer. Cancer Metastasis Rev. *31*, 469–478.

29. Tufegdzic Vidakovic, A., Rueda, O.M., Vervoort, S.J., Sati Batra, A., Goldgraben, M.A., Uribe-Lewis, S., Greenwood, W., Coffer, P.J., Bruna, A., and Caldas, C. (2015). Context-Specific Effects of TGF-β/SMAD3 in Cancer Are Modulated by the Epigenome. Cell Rep. *13*, 2480–2490.

30. Moffitt, R.A., Marayati, R., Flate, E.L., Volmar, K.E., Loeza, S.G., Hoadley, K.A., Rashid, N.U., Williams, L.A., Eaton, S.C., Chung, A.H., et al. (2015). Virtual microdissection identifies distinct tumor- and stroma-specific subtypes of pancreatic ductal adenocarcinoma. Nat. Genet. *47*, 1168–1178.

31. Sheffer, M., Bacolod, M.D., Zuk, O., Giardina, S.F., Pincas, H., Barany, F., Paty, P.B., Gerald, W.L., Notterman, D.A., and Domany, E. (2009). Association of survival and disease progression with chromosomal instability: a genomic exploration of colorectal cancer. Proc. Natl. Acad. Sci. USA *106*, 7131–7136.

32. Martin, M.L., Zeng, Z., Adileh, M., Jacobo, A., Li, C., Vakiani, E., Hua, G., Zhang, L., Haimovitz-Friedman, A., Fuks, Z., et al. (2018). Logarithmic expansion of LGR5^{+} cells in human colorectal cancer. Cell. Signal. *42*, 97–105.

33. Jin, F., Li, Y., Dixon, J.R., Selvaraj, S., Ye, Z., Lee, A.Y., Yen, C.A., Schmitt, A.D., Espinoza, C.A., and Ren, B. (2013). A high-resolution map of the three-dimensional chromatin interactome in human cells. Nature *503*, 290–294.

34. Szabowski, A., Maas-Szabowski, N., Andrecht, S., Kolbus, A., Schorpp-Kistner, M., Fusenig, N.E., and Angel, P. (2000). c-Jun and JunB antagonistically control cytokine-regulated mesenchymal-epidermal interaction in skin. Cell *103*, 745–755.

35. Ng, A.Y., Waring, P., Ristevski, S., Wang, C., Wilson, T., Pritchard, M., Hertzog, P., and Kola, I. (2002). Inactivation of the transcription factor Elf3 in mice results in dysmorphogenesis and altered differentiation of intestinal epithelium. Gastroenterology *122*, 1455–1466.

36. Jägle, S., Busch, H., Freihen, V., Beyes, S., Schrempp, M., Boerries, M., and Hecht, A. (2017). SNAIL1-mediated downregulation of FOXA proteins facilitates the inactivation of transcriptional enhancer elements at key epithelial genes in colorectal cancer cells. PLoS Genet. *13*, e1007109.

37. Isogaya, K., Koinuma, D., Tsutsumi, S., Saito, R.A., Miyazawa, K., Aburatani, H., and Miyazono, K. (2014). A Smad3 and TTF-1/NKX2-1 complex regulates Smad4-independent gene expression. Cell Res. *24*, 994–1008.

38. Johnstone, R.W., and Licht, J.D. (2003). Histone deacetylase inhibitors in cancer therapy: is transcription the primary target? Cancer Cell *4*, 13–18.

39. Tsai, J.H., and Yang, J. (2013). Epithelial-mesenchymal plasticity in carcinoma metastasis. Genes Dev. *27*, 2192–2206.

40. Massagué, J., and Obenauf, A.C. (2016). Metastatic colonization by circulating tumour cells. Nature *529*, 298–306.

41. Derksen, P.W., Liu, X., Saridin, F., van der Gulden, H., Zevenhoven, J., Evers, B., van Beijnum, J.R., Griffioen, A.W., Vink, J., Krimpenfort, P., et al. (2006). Somatic inactivation of E-cadherin and p53 in mice leads to metastatic lobular mammary carcinoma through induction of anoikis resistance and angiogenesis. Cancer Cell *10*, 437–449.

42. Qi, J., Nakayama, K., Cardiff, R.D., Borowsky, A.D., Kaul, K., Williams, R., Krajewski, S., Mercola, D., Carpenter, P.M., Bowtell, D., and Ronai, Z.A. (2010). Siah2-dependent concerted activity of HIF and FoxA2 regulates formation of neuroendocrine phenotype and neuroendocrine prostate tumors. Cancer Cell *18*, 23–38.

43. Estarás, C., Benner, C., and Jones, K.A. (2015). SMADs and YAP compete to control elongation of β-catenin:LEF-1-recruited RNAPII during hESC differentiation. Mol. Cell *58*, 780–793.

44. Beyer, T.A., Weiss, A., Khomchuk, Y., Huang, K., Ogunjimi, A.A., Varelas, X., and Wrana, J.L. (2013). Switch enhancers interpret TGF-β and Hippo signaling to control cell fate in human embryonic stem cells. Cell Rep. *5*, 1611–1624.

45. Zhu, C., Li, L., Zhang, Z., Bi, M., Wang, H., Su, W., Hernandez, K., Liu, P., Chen, J., Chen, M., et al. (2019). A non-canonical role of YAP/TEAD is required for activation of estrogen-regulated enhancers in breast cancer. Mol. Cell *75*, 791–806.e8.